

000 001 002 003 004 005 006 007 008 009 010 011 012 013 014 015 016 017 018 019 020 021 022 023 024 025 026 027 028 029 030 031 032 033 034 035 036 037 038 039 040 041 042 043 044 045 046 047 048 049 050 051 052 053 MARKOVIAN TRANSFORMERS FOR INFORMATIVE LANGUAGE MODELING

Anonymous authors

Paper under double-blind review

ABSTRACT

Chain-of-Thought (CoT) reasoning often fails to faithfully reflect a language model’s underlying decision process. We address this by introducing a *Markovian* language model framework that can be understood as a reasoning autoencoder: it creates a text-based bottleneck where CoT serves as an intermediate representation, forcing the model to compress essential reasoning into interpretable text before making predictions. We train this system with a GRPO-style policy gradient algorithm using parallel sampling, a frozen baseline CoT’, within-batch standardized advantages, and actor-reward (chain-rule) gradients. Our approach yields large gains on QA tasks (e.g., GSM8K: 20.7% → 54.5%; +33.8 pp; ARC-Challenge: 47.5% → 76.9%; +29.4 pp). Perturbation analyses across types and severities show consistently higher sensitivity to CoT edits (typically 52%–82% of cases favor Markovian), indicating stronger causal reliance on the CoT. Cross-model evaluation confirms that learned CoTs generalize across architectures, suggesting they capture transferable reasoning patterns rather than model-specific artifacts.

1 INTRODUCTION

The rapid advancement of language models (LMs) has led to impressive performance on complex cognitive tasks (Brown et al., 2020). Yet it is often unclear *why* an LM arrives at a particular conclusion (Lamparth & Reuel, 2023; Burns et al., 2023; Gurnee & Tegmark, 2024), causing issues in high-stakes applications (Grabb et al., 2024; Lamparth et al., 2024; Rivera et al., 2024). Traditional interpretability methods analyze hidden activations or attention patterns to extract “explanations” (Geiger et al., 2022; Geva et al., 2022; Meng et al., 2022; Casper et al., 2023; Wang et al., 2022; Lamparth & Reuel, 2023; Nanda et al., 2023). Modern LMs, however, already generate coherent text: we might hope *prompting* the model to articulate its reasoning (“Chain-of-Thought” or CoT) (Nye et al., 2022; Wei et al., 2022) would yield a faithful record of its thought process.

Unfortunately, CoT explanations can be *unfaithful*. For example, Turpin et al. (2023) show that spurious in-context biases often remain hidden in the CoT, and Lanham et al. (2023) find that altering CoT text may not affect the final answer. Such observations indicate that standard CoTs are not “load-bearing.”

In this work, we take a *pragmatic* approach to interpretability, focusing on *informativeness* over full faithfulness. Rather than insisting the CoT mirrors the model’s entire internal process, we require that *the CoT alone suffices to produce the final answer*. In other words, if we remove the original prompt and rely only on the CoT, the model should still reach the correct output. This makes the CoT *causally essential* and *fragile*: changing it necessarily alters the prediction.

What distinguishes our approach is the clear distinction between the model *relying on its CoT* versus generating *more informative CoTs*. While traditional approaches train models to generate better-quality CoTs, they don’t fundamentally change how the model uses them. Our Markovian framework, by contrast, forces the model to process information through the CoT bottleneck, making the CoT not just informative but *causally load-bearing* for prediction.

For instance, Llama’s CoT on arithmetic tasks changed dramatically after training. **Before training**, it simply listed all numbers and their (incorrect) sum (e.g., “Sum = 76 + 90 + 92 + ... = 2314”). **After training**, it performed correct step-by-step calculations (e.g., “calculate 6 + 89 = 95; Next, calculate

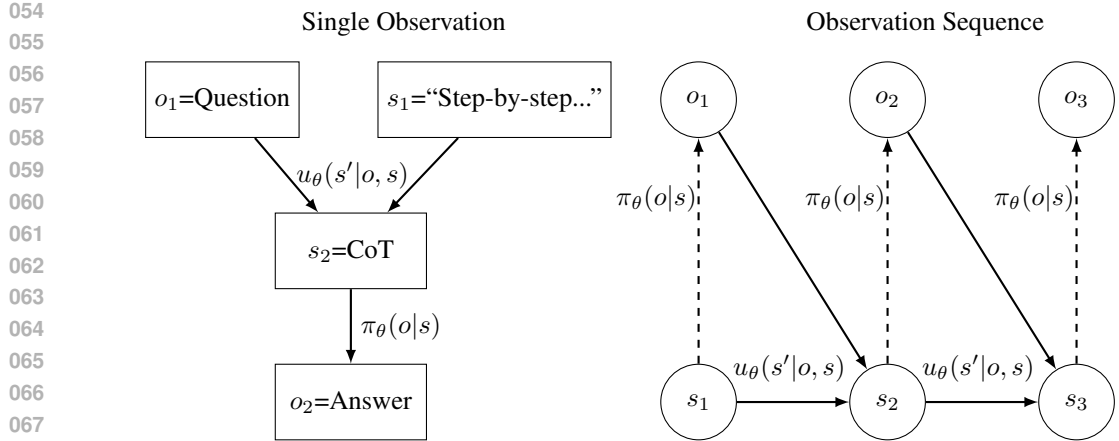


Figure 1: Markovian training as a reasoning autoencoder. Left: Single time-step process from Question to CoT to Answer, creating a text-based bottleneck where the CoT must capture all information needed for answer prediction. Right: Causal structure showing the generation of states from observations and previous states using the state update function $u_\theta(s'|o, s)$, and the prediction of observations from states using the policy $\pi_\theta(o|s)$. This architecture forces reasoning through an interpretable text bottleneck, but prevents direct backpropagation, necessitating RL-based gradient estimation.

95 + 38 = 133..."), breaking the task into manageable steps that can be verified independently and enabling accurate answer prediction even when the original question is removed.

Recipient-Specific Compression. A key insight is that an *informative* CoT can also serve as a *recipient-specific compression* of the model’s hidden knowledge: it distills the essential reasoning into text that another recipient (e.g. a different model or a human) can use to predict the same outcome. Our experiments confirm that the learned CoTs generalize across interpreters, suggesting that these textual explanations genuinely encode transferable problem-solving steps rather than model-specific quirks (Section 5.4).

Contributions.

1. We introduce a Markovian language model framework that structurally enforces CoT generation to be causally essential, ensuring reliance on the CoT for predictions.
2. We apply this framework to arithmetic problems (Mistral 7B) and the GSM8K dataset (Cobbe et al., 2021) (Llama 3.1 8B), observing a 33.2% absolute improvement on GSM8K.
3. We show through systematic perturbation analysis across four model pairs that Markovian training produces significantly higher sensitivity to CoT perturbations compared to Non-Markovian approaches, with effect differences ranging from +0.0154 to +0.3276 in log-probability sensitivity.
4. We demonstrate cross-model transfer: CoTs trained on one model remain informative for other models. This underscores the CoT’s *recipient-specific* interpretability and suggests it captures a shared reasoning strategy.

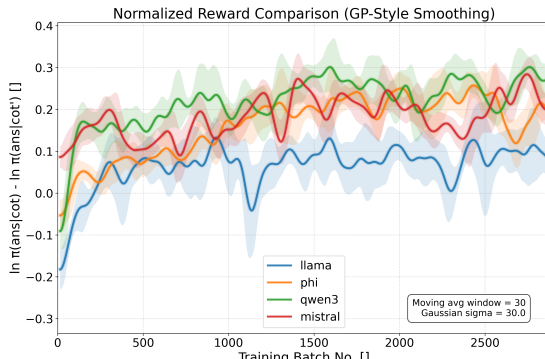
Section 2 reviews related work, Section 3 details our Markovian framework, and Section 4 describes the RL training. Section 5 presents empirical results, and Section 6 discusses limitations and future directions.

2 RELATED WORK

Prior work shows that CoT prompting can boost performance on reasoning tasks (Wei et al., 2022; Nye et al., 2022). Whereas typical CoT prompting methods do not alter a pre-trained model’s

Dataset	Before	After	Δ
GSM8K	20.70%	54.50%	+33.80 pp
MMLU	35.92%	32.40%	-3.52 pp
Arithmetic	5.50%	> 99%	≥ 93.50 pp
SVAMP	21.33%	35.00%	+13.67 pp
AQuA	16.54%	20.80%	+4.26 pp
ARC-Chal	47.46%	76.87%	+29.41 pp

(a) Llama scores across datasets (verbatim correct at T=0). Δ reports absolute percentage-point (pp) gains.



(b) Cross-model normalized reward

Figure 2: Left: dataset-wise performance for Llama before vs. after Markovian training. Scores are fractions of verbatim-correct answers at temperature 0; Δ is absolute percentage points. Right: normalized reward $\ln \pi_\theta(\text{ans} | \text{CoT}) - \ln \pi_\theta(\text{ans} | \text{CoT}')$ on Wikipedia continuation for multiple base models (Llama 3.1 8B, Phi-3.5 Mini, Qwen3 4B, Mistral 7B), showing consistent gains in CoT informativeness across architectures. Together, the table highlights robustness across datasets, while the plot highlights robustness across model families.

parameters, some prior approaches do fine-tune the model for CoT generation (Zelikman et al., 2022; 2024; DeepSeek-AI et al., 2025). Our work differs by removing the original question or passage from the answer-prediction context, which enforces a stronger causal reliance on the CoT.

Regarding faithfulness vs. interpretability, some authors discuss how a CoT may fail to reflect the true reason the LM arrived at its answer (Lanham et al., 2023; Turpin et al., 2023), since small changes in the CoT do not necessarily change the final prediction. Zhou et al. (2023) analyze CoT through an information-theoretic lens, finding that CoT can serve as a communication channel between different parts of a model. We build on these insights by *training* the model to rely on this channel exclusively.

Architecturally, our Markovian LM shares structural similarities with state space models like RNNs (Rumelhart et al., 1986), S4 (Gu et al., 2022), and Mamba (Gu & Dao, 2024), though with a key difference: MLMs have probabilistic state transitions to model token sampling, which necessitates gradient estimation methods such as policy gradient (Sutton et al., 1999) rather than direct backpropagation. This probabilistic structure also resembles Kalman filters (Å ström, 1965), Deep Variational Bayes Filters (Karl et al., 2017), Deep Kalman Filters (Krishnan et al., 2015), and Variational Recurrent Neural Networks (VRNN) (Chung et al., 2015), though we use categorical rather than Gaussian distributions for interpretable text generation. Other fine-tuned reasoning models mentioned above (R1, STaR, and QuietSTaR) have similar structure but allow seeing the full context before generating state/reasoning tokens, whereas our approach enforces a strict information bottleneck through the state.

Lyu et al. (2023) also consider restricting the model’s ability to see the original input while generating the final answer. Their approach, however, involves rewriting the question in a structured formal language or code that is then executed. Our approach uses natural language for the reasoning state to preserve interpretability across diverse tasks.

3 MARKOVIAN LANGUAGE MODELS AND INFORMATIVENESS

Here we provide our formalism for Markovian Language Models (MLMs) and define *informativeness*, which we use as a training objective within our novel structural framework.

162 3.1 MARKOVIAN LANGUAGE MODELS (MLM)
163

164 A traditional LM can attend to the entire context when predicting the next token. This makes it
 165 possible for an LM to disregard the CoT or only partially rely on it. We impose a stricter, *Markovian*
 166 structure¹:

167 **Definition 3.1** (Markovian LM). *A Markovian Language Model is a tuple $M = (\mathcal{O}, \mathcal{S}, \pi, u, s_1)$,
 168 where*

- 169 • \mathcal{O} is a set of observations (e.g., questions and answers in a QA task),
 170
- 171 • \mathcal{S} is a set of states (e.g., CoT reasoning text),
 172
- 173 • $\pi : \mathcal{S} \rightarrow \Delta(\mathcal{O})$ is a policy that predicts the next observation from the state alone,
 174
- 175 • $u : \mathcal{O} \times \mathcal{S} \rightarrow \Delta(\mathcal{S})$ is a state update function (produces CoT from question and initial
 176 prompt),
 177
- $s_1 \in \mathcal{S}$ is an initial state (starting CoT prompt).

178 For example, in a math reasoning task, $o_1 \in \mathcal{O}$ might be a question, $s_1 \in \mathcal{S}$ is an initial CoT prompt
 179 like “Let’s solve this step-by-step:”, $s_2 \in \mathcal{S}$ is the generated reasoning chain, and $o_2 \in \mathcal{O}$ is the
 180 answer. The key idea is that π can only see the CoT state s_2 when predicting o_2 , forcing the CoT
 181 to contain all needed information. Intuitively, π is the next-token predictor, and u chooses how to
 182 produce the CoT from the latest observation and prior state. In our experiments, π and u are the
 183 same underlying transformer.

184 3.2 DATA-GENERATING DISTRIBUTION AND REWARD
185

186 Let P be the distribution over observations $x_1, x_2, \dots, x_T \in \mathcal{O}$. A trajectory τ is generated by:

$$187 \quad s_{t+1} \sim u(s_t, x_t), \quad x_{t+1} \sim P(x_{t+1} | x_{\leq t}),$$

188 with s_1 a fixed initial prompt. We define the *reward* for a trajectory τ as:

$$189 \quad R_\theta(\tau) = \sum_{t=1}^T [\ln \pi_\theta(x_t | s_t) - \ln \pi_\theta(x_t | s'_t)],$$

190 where s'_t is generated by a *baseline* update function u' , e.g., the *untrained* model. In words, $R_\theta(\tau)$
 191 measures how much more likely the correct observation x_t is under the trained state s_t compared to
 192 the baseline state s'_t .

193 3.3 INFORMATIVENESS OBJECTIVE
194

195 Conceptually, we aim to ensure that the CoT state serves as a critical bottleneck for information flow,
 196 making it causally essential for predictions. Formalizing this within our Markovian framework, we
 197 define:

$$201 \quad J(\theta) = \mathbb{E}_{\tau \sim P, u_\theta, u'} [R_\theta(\tau)],$$

202 where θ parameterizes u_θ . Maximizing $J(\theta)$ ensures that the update function u_θ produces states
 203 s_t that are *informative* about future observations (relative to the baseline u'), thereby enforcing the
 204 CoT’s role as a load-bearing component. We optimize $J(\theta)$ with policy gradient or PPO, sampling
 205 observations from P and states from u_θ and u' .

206 4 METHODS
207208 4.1 IMPLEMENTATION AS QUESTION-ANSWER PAIRS
209

210 In many tasks like math problem solving, we have $T = 2$ observations (question and answer) and
 211 implement the abstract MLM with a fixed maximum length for the CoT state. Let \mathcal{V} be a token

212 ¹This structure can be viewed as a stochastic variant of a Moore machine where both the transition function
 213 (u) and output function (π) are probabilistic, and the input and output alphabets are identical (\mathcal{O}). Alternatively,
 214 an MLM can be formalized as an F-coalgebra where $F(S) = P(O) \times P(S)^\mathcal{O}$, with P representing probability
 215 distributions.

vocabulary. We set $\mathcal{O} = \mathcal{V}^N$ and $\mathcal{S} = \mathcal{V}^K$ for some $N, K \in \mathbb{N}$, where K is the maximum tokens in the CoT. Note that while we limit the state to a maximum of K tokens for implementation, we do not enforce fixed-length observations.

Our conceptual arguments rely on $K < N$, as otherwise the model could simply write the predicted observation into the state. We satisfy this in our Wikipedia experiments (Sec 5.2), and for other experiments we find empirically that the model does not learn this undesirable behavior due to the difficulty of predicting the answer directly without any CoT.

In this setting, we denote our states as $s_1 = \text{CoT}_{\text{init}}$ and $s_2 = \text{CoT}$, where CoT_{init} is a task-specific prompt². With pre-trained LM \mathcal{L} , we can implement our update function u and policy π using:

$$\begin{aligned} \ln u_{\theta}(s_2 = \text{CoT} \mid q, s_1 = \text{CoT}_{\text{init}}) &= \sum_{i=1}^K \ln \mathcal{L}_{\theta}(\text{concat}(q, \text{CoT}_{\text{init}}, \text{CoT}_{<i}))[\text{CoT}_i], \\ \ln \pi_{\theta}(\text{ans} \mid \text{CoT}) &:= \sum_{i=1}^N \ln \mathcal{L}_{\theta}(\text{concat}(\text{CoT}, \text{ans}_{<i}))[\text{ans}_i]. \end{aligned}$$

Compression viewpoint. Our "CoT as compression" narrative applies most directly to continuation tasks (e.g., Wikipedia), where the content to be predicted is longer than the CoT, forcing the model to compress salient context into a short textual bottleneck. For QA tasks, the answer is typically shorter than the CoT; there we emphasize the CoT's *sufficiency and fragility* rather than literal compression, and use QA as evidence that the training method generalizes across task types.

Crucially, we do *not* allow the answer generation to attend back to the question q directly; the question is replaced by the CoT. For each question q , we generate the baseline state s'_2 (which we denote as CoT' in this setting) by prompting the unmodified pre-trained model with q plus an initial instruction (e.g., 'Think step-by-step...'), and recording its raw output.

Our reward is:

$$R_{\theta} = \ln \pi_{\theta}(\text{ans} \mid \text{CoT}) - \ln \pi_{\theta}(\text{ans} \mid \text{CoT}').$$

4.2 POLICY GRADIENT WITH GRPO-STYLED BASELINE

Markovian training can be understood as training a *reasoning autoencoder*, where the CoT serves as a text-based bottleneck between question and answer. Like traditional autoencoders, this architecture forces information compression, but the intermediate representation is interpretable text rather than latent vectors. This text bottleneck prevents direct backpropagation and necessitates reinforcement learning techniques for gradient estimation.

4.2.1 ACTOR REWARD GRADIENTS: THE KEY INNOVATION

Our approach differs fundamentally from standard reinforcement learning by using the *same* transformer with weights θ as both the policy model and the reward model. This creates a crucial mathematical distinction from traditional policy gradient methods.

In classical policy gradient, the reward $R(\tau)$ is independent of the policy parameters, leading to the standard REINFORCE gradient:

$$\nabla_{\theta} \mathbb{E}_{\tau \sim P_{\theta}}[R(\tau)] = \mathbb{E}_{\tau \sim P_{\theta}}[R(\tau) \cdot \nabla_{\theta} \ln P_{\theta}(\tau)]$$

However, in our case, the reward is a function of the same parameters: $R_{\theta}(\tau) = \ln \pi_{\theta}(\text{ans} \mid \text{CoT})$. Applying the chain rule:

$$\nabla_{\theta} \mathbb{E}_{\tau \sim P_{\theta}}[R_{\theta}(\tau)] = \mathbb{E}_{\tau \sim P_{\theta}}[R_{\theta}(\tau) \nabla_{\theta} \ln P_{\theta}(\tau) + \nabla_{\theta} R_{\theta}(\tau)].$$

This yields two terms: the standard policy gradient ($R_{\theta}(\tau) \cdot \nabla_{\theta} \ln P_{\theta}(\tau)$) and the direct reward gradient ($\nabla_{\theta} R_{\theta}(\tau)$). We include both terms with equal weight in our implementation.

²The exact prompt template varies by task type, with each template specifying the task objective, allowed CoT length, and an invitation to reason strategically. Full templates are provided in Sec A.

270 4.2.2 GRPO-STYLE BASELINE WITH LOCAL SUBTRACTION
271

272 We implement a policy gradient algorithm inspired by Group Relative Policy Optimization (GRPO),
273 originally introduced by Shao et al. Shao et al. (2024) in DeepSeek-Math. GRPO eliminates the
274 critic model from PPO by using group-based advantage estimation, where multiple responses to the
275 same query provide relative baselines for each other.

276 However, we add an additional baseline subtraction step before applying GRPO’s batch averaging.
277 We first compute a local baseline using the frozen reference model u' , then apply GRPO-style
278 standardization within each batch.
279

280 4.2.3 PARALLEL SAMPLING STRATEGY
281

282 We employ *parallel sampling* (inspired by GRPO): each training batch contains B copies of the
283 same question-answer pair (q, a) . The trainable model u_θ generates diverse reasoning chains
284 $\{\text{CoT}_1, \text{CoT}_2, \dots, \text{CoT}_B\}$ for the identical input through stochastic sampling.

285 Additionally, we introduce a frozen baseline from the reasoning autoencoder: the unmodified model
286 u' generates a single reference CoT' that provides a local baseline before applying GRPO-style
287 batch averaging. This frozen baseline represents the “encoder” component of our reasoning autoen-
288 coder—capturing the model’s initial reasoning ability before training. The frozen baseline CoT' is
289 *not* part of the original GRPO algorithm—it is our contribution to provide a more stable reference
290 point.

291 This approach provides several advantages:
292

- **Reasoning bottleneck:** The CoT' baseline establishes the initial encoding capacity of the reasoning autoencoder
- **Local baseline:** The frozen CoT' provides a consistent reference for measuring informativeness improvement
- **Computational efficiency:** Baseline reasoning and answer evaluation are computed once and replicated
- **Stable variance estimation:** All samples share the same ground truth, enabling robust within-batch standardization

303 4.2.4 IMPLEMENTATION: TWO-TERM LOSS FUNCTION
304

305 Our implementation combines both gradient terms from the chain rule derivation above. The loss
306 function includes:
307

$$\mathcal{L} = \mathcal{L}_{\text{PG}} + \mathcal{L}_{\text{AR}}, \quad \mathcal{L}_{\text{PG}} = -\ln u_\theta(\text{CoT} \mid q, \text{CoT}_{\text{init}}) \cdot A^{\text{detach}}, \quad \mathcal{L}_{\text{AR}} = -A.$$

308 where A is the standardized advantage (after local baseline subtraction and GRPO-style batch aver-
309 aging) and A^{detach} blocks gradients to isolate the policy gradient term.
310

311 The first term \mathcal{L}_{PG} corresponds to the standard REINFORCE gradient $A_\theta(\tau) \cdot \nabla_\theta \ln P_\theta(\tau)$, while the
312 second term \mathcal{L}_{AR} corresponds to the direct advantage gradient $\nabla_\theta A_\theta(\tau)$. This enables simultaneous
313 optimization of CoT generation and answer prediction.
314

315 4.2.5 WITHIN-BATCH ADVANTAGE STANDARDIZATION
316

317 Instead of historical exponential moving averages, we standardize advantages within each batch:
318

$$R_i = \ln \pi_\theta(\text{ans} \mid \text{CoT}_i) - \ln \pi_\theta(\text{ans} \mid \text{CoT}'), \quad A_i = \frac{R_i - \mu_{\text{batch}}}{\sigma_{\text{batch}} + \epsilon}.$$

319 where $\mu_{\text{batch}} = \frac{1}{B} \sum_{i=1}^B R_i$ and $\sigma_{\text{batch}}^2 = \frac{1}{B} \sum_{i=1}^B (R_i - \mu_{\text{batch}})^2$.
320

321 This ensures that advantages have zero mean and unit variance within each batch, providing stable
322 gradients regardless of the absolute reward scale.
323

324 **Algorithm 1** Markovian Training with GRPO-Style Batch Baseline

325
326 1: Given dataset P of (q, a) , trainable actor u_θ , frozen baseline u' , answer policy π_θ , batch size B
327 2: **for** each training batch **do**
328 3: Sample $(q, a) \sim P$
329 4: Sample $\text{CoT}_i \sim u_\theta(\cdot | q, \text{CoT}_{\text{init}})$ for $i = 1..B$ (stochastic parallel sampling)
330 5: Sample baseline $\text{CoT}' \sim u'(\cdot | q, \text{CoT}_{\text{init}})$ (once per batch)
331 6: Compute actor answer log-probs $r_i = \ln \pi_\theta(a | \text{CoT}_i)$
332 7: Compute baseline log-prob $b = \ln \pi_\theta(a | \text{CoT}')$
333 8: Normalized rewards $R_i = r_i - b$; standardize within-batch: $A_i = \frac{R_i - \mu}{\sigma + \epsilon}$
334 9: Policy gradient loss: $\ell_i^{\text{PG}} = -\ln u_\theta(\text{CoT}_i | q, \text{CoT}_{\text{init}}) \cdot A_i^{\text{detach}}$
335 10: Actor-reward gradient: $\ell_i^{\text{AR}} = -A_i$
336 11: Optional KL penalty: $\ell_i^{\text{KL}} = 0.1 D_{KL}(u_\theta(\cdot | q) \| u'(\cdot | q))$
337 12: Total loss: $\ell_i = \ell_i^{\text{PG}} + \ell_i^{\text{AR}} + \ell_i^{\text{KL}}$; update θ with $\frac{1}{B} \sum_i \ell_i$
338 13: **end for**

339
340 **5 EXPERIMENTS**

343 We evaluate in two regimes: (i) continuation (Wikipedia), where CoT tokens act as a lossy com-
344 pression of longer context, and (ii) question–answer datasets (GSM8K, MMLU, SVAMP, AQuA,
345 ARC, Arithmetic), which validate the general-purpose efficacy of Markovian training even when
346 the “compression” story is not literal.

347
348 **5.1 QUESTION–ANSWER TASKS (GSM8K, MMLU, SVAMP, AQUA, ARC, ARITHMETIC)**

349 We evaluate on standard QA-style datasets (GSM8K (Cobbe et al., 2021), MMLU (Hendrycks et al.,
350 2020), SVAMP (Patel et al., 2021), AQuA (Ling et al., 2017), ARC Challenge (Clark et al., 2018),
351 and our non-standard multi-step addition task. All QA experiments use the same optimization:
352 GRPO-style parallel sampling with within-batch standardization and the chain-rule reward (policy-
353 gradient plus actor-reward gradient), with task-specific default CoT lengths. For arithmetic, each
354 problem has fifteen random terms in $[1, 99]$; the model learns to produce step-wise reasoning and
355 achieves $> 99\%$ verbatim-correct answers at $T=0$.

356
357 **CoT length defaults.** Unless otherwise specified, we use: GSM8K 100, Arithmetic 150,
358 Arithmetic-Negative 150, MMLU 150. See §4 for objective details.

360 **5.2 WIKIPEDIA CONTINUATION**

362 For Wikipedia continuation (Foundation, 2024), we condition on the first 200 tokens and predict the
363 next 100 tokens, allowing 50 tokens of CoT. Training uses the same GRPO with chain-rule reward
364 as in QA. We observe improvements consistent with increased CoT informativeness (cf. Fig. 2), and
365 §5.3 shows stronger perturbation sensitivity under Markovian training.

366
367 **5.3 MARKOVIAN VS NON-MARKOVIAN PERTURBATION SENSITIVITY**

368 To provide systematic evidence for the theoretical advantages of Markovian training, we conduct
369 comprehensive perturbation sensitivity comparisons between Markovian and Non-Markovian model
370 pairs. The Non-Markovian models are trained using the same hyperparameters, only differing in that
371 the reward is $\pi_\theta(\text{ans} | q, \text{CoT})$ instead of $\pi_\theta(\text{ans} | \text{CoT})$. This analysis directly evaluates whether
372 the structural constraints in Markovian training lead to measurably different robustness properties
373 during training.

374
375 **5.3.1 EXPERIMENTAL DESIGN**

376
377 We measure perturbation sensitivity by evaluating fixed Markovian and Non-Markovian checkpoints
on newly sampled Wikipedia examples, regenerating actor CoTs for both models on the same inputs

Perturbation Type	Degree	Mean Effect Difference	Overall Consistency	Total Comparisons
Delete	20%	+0.0144	51.6%	128
	40%	+0.0513	65.6%	128
	60%	+0.0719	74.2%	128
	80%	+0.0986	78.1%	128
	100%	+0.1210	82.0%	128
Truncate Front	20%	-0.0028	42.2%	128
	40%	+0.0190	56.2%	128
	60%	+0.0355	63.3%	128
	80%	+0.0648	76.6%	128
	100%	+0.0983	81.2%	128
Truncate Back	20%	-0.0065	39.8%	128
	40%	+0.0010	47.7%	128
	60%	+0.0204	50.8%	128
	80%	+0.0473	62.5%	128
	100%	+0.0841	70.3%	128
Character Replace	20%	+0.0115	53.1%	128
	40%	+0.0488	62.5%	128
	60%	+0.0529	62.5%	128
	80%	+0.0504	62.5%	128
	100%	+0.0482	64.1%	128

Table 1: Fresh perturbation comparison between Markovian and Non-Markovian models using fixed checkpoints (adapter index 400) evaluated on 128 newly sampled Wikipedia continuation examples per perturbation type and degree. **Mean Effect Difference** is the average of (Markovian Effect – Non-Markovian Effect), where Effect is defined as $\ln P(\text{ans} \mid \text{CoT}_{\text{orig}}) - \ln P(\text{ans} \mid \text{CoT}_{\text{pert}})$. **Consistency** is the percentage of examples where the effect difference is positive (Markovian more sensitive).

before computing effects. We test four perturbation types at five severities (20%, 40%, 60%, 80%, 100%):

- **Delete:** Random token deletion from CoT reasoning
- **Truncate Front:** Removal of tokens from CoT beginning
- **Truncate Back:** Removal of tokens from CoT end
- **Character Replace:** Random character substitution within tokens

The sensitivity measure matches the implementation:

$$\text{Effect}_{\text{M/NM}} = \ln P(\text{ans} \mid \text{CoT}_{\text{original}}) - \ln P(\text{ans} \mid \text{CoT}_{\text{perturbed}}) \quad (1)$$

$$\text{Difference} = \text{Effect}_{\text{Markovian}} - \text{Effect}_{\text{Non-Markovian}} \quad (2)$$

Positive differences indicate greater Markovian sensitivity to CoT perturbations, reflecting stronger reliance on CoT integrity.

5.3.2 RESULTS SUMMARY

On 128 fresh Wikipedia examples per perturbation type, we find: Delete shows the strongest differences (mean +0.014 to +0.121 with 52%–82% consistency increasing with severity). Truncations start near zero or slightly negative at low severities and become positive with higher severities. Character replacement is consistently positive (+0.011 to +0.053; 63% consistency at higher severities).

5.4 INTERPRETABILITY OF COT GENERATIONS

To probe how well the reasoning generalizes, we evaluated the informativeness of Llama’s trained CoTs with respect to various other language models on the Wikipedia dataset. Cross-model evaluation shows strong correlation between improvements in both the trained model’s and alternative models’ evaluations of CoT quality throughout training. The normalized log probabilities increase simultaneously across different architectures, demonstrating that Llama is learning to produce

generic CoTs which do not over-fit to the peculiarities of a Llama answer-predictor. Results averaged across 6 independent training runs confirm this pattern holds consistently.

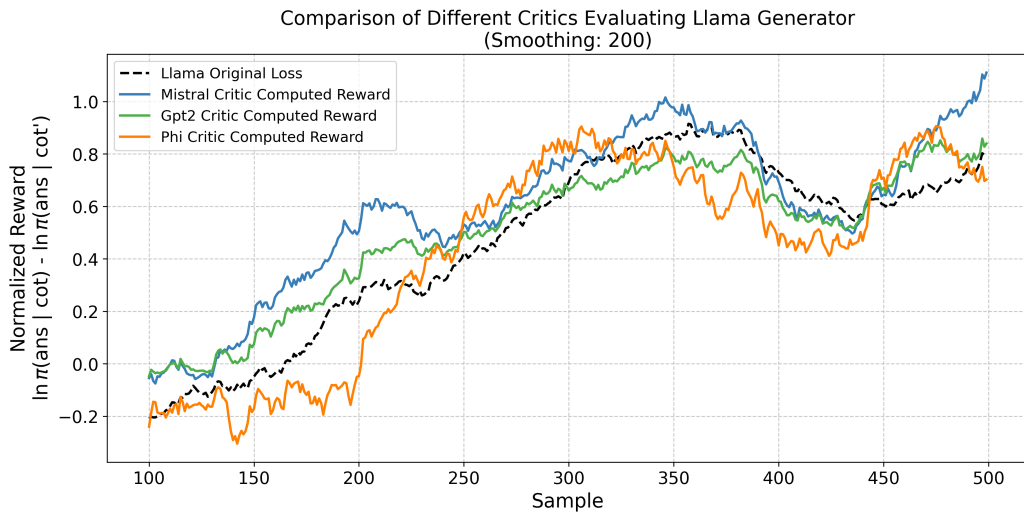


Figure 3: Cross-model evaluation comparing how different models (Mistral, GPT2, and Phi 3.5 Mini Instruct) utilize Llama 8B’s CoT on GSM8K. Results averaged across 3 training runs with smoothing window of 40.

This cross-model transferability addresses a key question: “interpretable to whom?” We test across three distinct model families (Phi (Abdin et al., 2024), Mistral, and GPT2), including GPT2, a significantly smaller model that shouldn’t be able to decode sophisticated steganography. The fact that trained CoTs transfer effectively across this diverse set confirms they contain generalizable reasoning patterns rather than model-specific artifacts. Note that the “CoT-as-compression” interpretation is specific to continuation settings; in QA, our gains indicate that enforcing a load-bearing, sufficient CoT improves reasoning utility even without a strict compression constraint.

6 DISCUSSION AND LIMITATIONS

Experiments across arithmetic, GSM8K, and Wikipedia show that it is possible to learn informative and interpretable CoT reasoning via RL on an LM using Markovian training.

We currently verify interpretability on myopic QA and continuation settings. A direct human study could further validate whether CoTs are genuinely human-interpretable beyond our model-centric proxies (fragility and cross-model transfer). Nonetheless, we observe substantial gains in CoT fragility and cross-model transfer, suggesting practical opportunities for improved interpretability. The Markovian design also naturally extends to multi-turn dialogue by treating the CoT as a recurrent state; after each user message o_t we produce the next CoT s_{t+1} via $u_\theta(s_{t+1} \mid s_t, o_t)$ and generate the system’s reply from s_{t+1} alone. We leave multi-turn evaluation to future work.

486 **7 REPRODUCIBILITY STATEMENT**
 487

488 To ensure reproducibility, we provide comprehensive supplementary materials including all source
 489 code, training and evaluation scripts, and detailed instructions in the README. The main training
 490 loop (`src/train.py`) supports (i) GRPO, and alternate training methods such as EI, PG, and
 491 PPO-style clipped objective methods (see Section F for detailed algorithm descriptions) and (ii) all
 492 experimental datasets. We measure fragility of CoT via `src/perturbation_analysis.py`
 493 and we estimate interpretability of CoT generations via `src/evaluate_cross_model.py`.

494 Complete hyperparameter configurations for all Wikipedia continuation experiments are provided
 495 in Table 2.

496 **Models:** We support 11 language model architectures with full tokenization and formatting: Llama
 497 3.1 8B Instruct, Llama 3.2 1B Instruct, Mistral 7B Instruct V0.2, GPT-2 (124M), TinyStories (33M),
 498 Phi 3.5 Mini Instruct, Phi-4, Qwen3 4B, Qwen3 14B, Gemma-3 2B, and Gemma-3 Small (9B). All
 499 models use public HuggingFace implementations with LoRA fine-tuning.

500 **Datasets:** We support the following task types: (1) *arithmetic* - randomly generated 15-term addition
 501 problems, (2) *arithmetic-negative* - addition with negative numbers, (3) *GSM8K* (Cobbe et al.,
 502 2021), (4) *MMLU* (Hendrycks et al., 2020), (5) *SVAMP* (Patel et al., 2021), (6) *AQuA* (Ling et al.,
 503 2017), (7) *ARC-Challenge* (Clark et al., 2018), (8) *wiki_compression* - predicting repeated Wikipedia
 504 text, and (9) *wiki_continuation* - next-token prediction on Wikipedia articles. Environment setup in-
 505 structions are provided in the README.

506 Our experiments were conducted on NVIDIA H100 and H200 GPUs through the RunPod cloud service.
 507 We trained and evaluated across multiple tasks and settings, including: QA datasets (GSM8K,
 508 MMLU, SVAMP, AQuA, ARC-Challenge; §5.1), the non-standard multi-step addition task (§5.1),
 509 and Wikipedia continuation (§5.2). We also ran systematic perturbation sensitivity studies (§5.3),
 510 cross-model evaluations (Fig. 3), and hyperparameter/model sweeps (Table 2) across Llama, Mis-
 511 tral, Phi, and Qwen3, and temperatures 1.2/1.3/1.4. We tried various other architectures includ-
 512 ing straight-through estimators through token sampling and the Decision Transformer (Chen et al.,
 513 2021). Taken together, these experiments required substantial compute; the total compute for the
 514 reported experiments was approximately 10,000 GPU-hours. The broader research project, includ-
 515 ing preliminary runs and ablations not reported here, consumed approximately \$32,000 in cloud
 516 resources. We provide these figures to help researchers anticipate the resources needed to reproduce
 517 and extend our results.

518 With these materials, researchers should be able to reproduce our work, including the performance
 519 boost on GSM8K and the perturbation analysis results demonstrating CoT reliance.

521 **REFERENCES**

523 Karl Johan Å ström. Optimal control of markov processes with incomplete state information i, 1965.

525 Marah Abdin, Jyoti Aneja, Hany Awadalla, Ahmed Awadallah, Ammar Ahmad Awan, Nguyen
 526 Bach, Amit Bahree, Arash Bakhtiari, Jianmin Bao, et al. Phi-3 technical report: A highly capable
 527 language model locally on your phone, 2024.

529 Yuntao Bai, Saurav Kadavath, Sandipan Kundu, Amanda Askell, Jackson Kernion, Andy Jones,
 530 Anna Chen, Anna Goldie, Azalia Mirhoseini, Cameron McKinnon, Carol Chen, Catherine Ols-
 531 son, Christopher Olah, Danny Hernandez, Dawn Drain, Deep Ganguli, Dustin Li, Eli Tran-
 532 Johnson, Ethan Perez, Jamie Kerr, Jared Mueller, Jeffrey Ladish, Joshua Landau, Kamal Ndousse,
 533 Kamile Lukosuite, Liane Lovitt, Michael Sellitto, Nelson Elhage, Nicholas Schiefer, Noemi Mer-
 534 cado, Nova DasSarma, Robert Lasenby, Robin Larson, Sam Ringer, Scott Johnston, Shauna
 535 Kravec, Sheer El Showk, Stanislav Fort, Tamera Lanham, Timothy Telleen-Lawton, Tom Con-
 536 erly, Tom Henighan, Tristan Hume, Samuel R. Bowman, Zac Hatfield-Dodds, Ben Mann, Dario
 537 Amodei, Nicholas Joseph, Sam McCandlish, Tom Brown, and Jared Kaplan. Constitutional ai:
 538 Harmlessness from ai feedback, 2022.

539 Tom Brown, Benjamin Mann, Nick Ryder, Melanie Subbiah, Jared D Kaplan, Prafulla Dhariwal,
 et al. Language models are few-shot learners, 2020.

- 540 Collin Burns, Haotian Ye, Dan Klein, and Jacob Steinhardt. Discovering latent knowledge in lan-
 541 guage models without supervision, 2023.
- 542
- 543 Stephen Casper, Tilman Rauker, Anson Ho, and Dylan Hadfield-Menell. Sok: Toward transparent
 544 ai: A survey on interpreting the inner structures of deep neural networks, 2023.
- 545
- 546 Lili Chen, Kevin Lu, Aravind Rajeswaran, Kimin Lee, Aditya Grover, Michael Laskin, Pieter
 547 Abbeel, Aravind Srinivas, and Igor Mordatch. Decision transformer: Reinforcement learning
 548 via sequence modeling. In *Advances in Neural Information Processing Systems*, 2021.
- 549
- 550 Paul Christiano, Ajeya Cotra, and Mark Xu. Eliciting latent knowledge: How to tell if your eyes
 551 deceive you, 2021.
- 552
- 553 Paul Christiano, Jan Leike, Tom B. Brown, Miljan Martic, Shane Legg, and Dario Amodei. Deep
 554 reinforcement learning from human preferences, 2023.
- 555
- 556 Junyoung Chung, Kyle Kastner, Laurent Dinh, Kratarth Goel, Aaron C. Courville, and Yoshua Ben-
 557 gio. A recurrent latent variable model for sequential data, 2015.
- 558
- 559 Peter Clark, Isaac Cowhey, Oren Etzioni, Tushar Khot, Ashish Sabharwal, Carissa Schoenick, and
 560 Oyvind Tafjord. Think you have solved question answering? try arc, the ai2 reasoning challenge.
 561 In *Proceedings of the 2018 Workshop on Machine Reading for Question Answering*, 2018.
- 562
- 563 Karl Cobbe, Vineet Kosaraju, Mohammad Bavarian, Mark Chen, Heewoo Jun, Lukasz Kaiser,
 564 Matthias Plappert, Jerry Tworek, Jacob Hilton, Reiichiro Nakano, Christopher Hesse, and John
 565 Schulman. Training verifiers to solve math word problems, 2021.
- 566
- 567 DeepSeek-AI, Daya Guo, Dejian Yang, Haowei Zhang, Junxiao Song, Ruoyu Zhang, Runxin Xu,
 568 et al. Deepseek-r1: Incentivizing reasoning capability in llms via reinforcement learning, 2025.
- 569
- 570 Wikimedia Foundation. Wikipedia, 2024.
- 571
- 572 Atticus Geiger, Zhengxuan Wu, Hanson Lu, Josh Rozner, Elisa Kreiss, Thomas Icard, Noah Good-
 573 man, and Christopher Potts. Inducing causal structure for interpretable neural networks, 2022.
- 574
- 575 Mor Geva, Avi Caciularu, Kevin Ro Wang, and Yoav Goldberg. Transformer feed-forward layers
 576 build predictions by promoting concepts in the vocabulary space, 2022.
- 577
- 578 Declan Grabb, Max Lamparth, and Nina Vasan. Risks from language models for automated mental
 579 healthcare: Ethics and structure for implementation, 2024.
- 580
- 581 Albert Gu and Tri Dao. Mamba: Linear-time sequence modeling with selective state spaces, 2024.
- 582
- 583 Albert Gu, Karan Goel, and Christopher Ré. Efficiently modeling long sequences with structured
 584 state spaces, 2022.
- 585
- 586 Wes Gurnee and Max Tegmark. Language models represent space and time, 2024.
- 587
- 588 Dan Hendrycks, Collin Burns, Steven Basart, Andy Zou, Mantas Mazeika, Dawn Song, and
 589 Jacob Steinhardt. Measuring massive multitask language understanding. *arXiv preprint*
 590 *arXiv:2009.03300*, 2020.
- 591
- 592 Edward J Hu, Yelong Shen, Phillip Wallis, Zeyuan Allen-Zhu, Yuanzhi Li, Shean Wang, Lu Wang,
 593 and Weizhu Chen. Lora: Low-rank adaptation of large language models, 2022.
- 594
- 595 Nitish Joshi, Javier Rando, Abulhair Saparov, Najoung Kim, and He He. Personas as a way to model
 596 truthfulness in language models, 2024.
- 597
- 598 Maximilian Karl, Maximilian Soelch, Justin Bayer, and Patrick van der Smagt. Deep variational
 599 bayes filters: Unsupervised learning of state space models from raw data, 2017.
- 600
- 601 Rahul G. Krishnan, Uri Shalit, and David Sontag. Deep kalman filters, 2015.
- 602
- 603 Max Lamparth and Anka Reuel. Analyzing and editing inner mechanisms of backdoored language
 604 models, 2023.

- 594 Max Lamparth, Anthony Corso, Jacob Ganz, Oriana Skylar Mastro, Jacquelyn Schneider, and
 595 Harold Trinkunas. Human vs. machine: Language models and wargames, 2024.
 596
- 597 Tamera Lanham, Anna Chen, Ansh Radhakrishnan, Benoit Steiner, Carson Denison, Danny Her-
 598 nandez, Dustin Li, Esin Durmus, Evan Hubinger, Jackson Kernion, Kamilé Lukošiūtė, Karina
 599 Nguyen, Newton Cheng, Nicholas Joseph, Nicholas Schiefer, Oliver Rausch, Robin Larson,
 600 Sam McCandlish, Sandipan Kundu, Saurav Kadavath, Shannon Yang, Thomas Henighan, Tim-
 601 othy Maxwell, Timothy Telleen-Lawton, Tristan Hume, Zac Hatfield-Dodds, Jared Kaplan, Jan
 602 Brauner, Samuel R. Bowman, and Ethan Perez. Measuring faithfulness in chain-of-thought rea-
 603 soning, 2023.
- 604 Stephanie Lin, Jacob Hilton, and Owain Evans. Truthfulqa: Measuring how models mimic human
 605 falsehoods, 2022.
- 606 Wang Ling, Dani Yogatama, Chris Dyer, and Phil Blunsom. Program induction by rationale gener-
 607 ation: Learning to solve and explain algebraic word problems. In *Proceedings of the 55th Annual*
 608 *Meeting of the Association for Computational Linguistics (ACL)*, 2017.
- 609
- 610 Qing Lyu, Shreya Havaldar, Adam Stein, Li Zhang, Delip Rao, Eric Wong, Marianna Apidianaki,
 611 and Chris Callison-Burch. Faithful chain-of-thought reasoning, 2023.
- 612 Kevin Meng, David Bau, Alex J Andonian, and Yonatan Belinkov. Locating and editing factual
 613 associations in gpt, 2022.
- 614
- 615 Neel Nanda, Lawrence Chan, Tom Lieberum, Jess Smith, and Jacob Steinhardt. Progress measures
 616 for grokking via mechanistic interpretability, 2023.
- 617
- 618 Maxwell Nye, Anders Johan Andreassen, Guy Gur-Ari, Henryk Michalewski, Jacob Austin, David
 619 Bieber, David Dohan, Aitor Lewkowycz, Maarten Bosma, David Luan, Charles Sutton, and Au-
 620 gustus Odena. Show your work: Scratchpads for intermediate computation with language models,
 621 2022.
- 622 Prateek Patel, Satwik Bhattacharya, and Navin Goyal. Are nlp models really robust? a case study
 623 on numerical reasoning. In *Proceedings of the 2021 Conference on Empirical Methods in Natural*
 624 *Language Processing*, 2021.
- 625 Juan-Pablo Rivera, Gabriel Mukobi, Anka Reuel, Max Lamparth, Chandler Smith, and Jacquelyn
 626 Schneider. Escalation risks from language models in military and diplomatic decision-making,
 627 2024.
- 628
- 629 David E. Rumelhart, Geoffrey E. Hinton, and Ronald J. Williams. Learning representations by
 630 back-propagating errors, 1986.
- 631 Zhihong Shao, Peiyi Wang, Qihao Zhu, Runxin Xu, Junxiao Song, Xiao Bi, Haowei Zhang,
 632 Mingchuan Zhang, Y.K. Li, Y. Wu, and Daya Guo. Deepseekmath: Pushing the limits of mathe-
 633 matical reasoning in open language models, 2024.
- 634
- 635 D. Silver, A. Huang, C. Maddison, et al. Mastering the game of go with deep neural networks and
 636 tree search, 2016.
- 637
- 638 David Silver, Thomas Hubert, Julian Schrittwieser, Ioannis Antonoglou, Matthew Lai, Arthur Guez,
 639 Marc Lanctot, Laurent Sifre, Dharmshan Kumaran, Thore Graepel, Timothy Lillicrap, Karen Si-
 640 monyan, and Demis Hassabis. Mastering chess and shogi by self-play with a general reinforce-
 641 ment learning algorithm, 2017.
- 642
- 643 Richard S. Sutton, David McAllester, Satinder Singh, and Yishay Mansour. Policy gradient methods
 644 for reinforcement learning with function approximation, 1999.
- 645
- Katherine Tian, Eric Mitchell, Huaxiu Yao, Christopher D. Manning, and Chelsea Finn. Fine-tuning
 646 language models for factuality, 2023.
- 647 Miles Turpin, Julian Michael, Ethan Perez, and Samuel R. Bowman. Language models don't always
 say what they think: Unfaithful explanations in chain-of-thought prompting, 2023.

648 Kevin Ro Wang, Alexandre Variengien, Arthur Conmy, Buck Shlegeris, and Jacob Steinhardt. In-
 649 terpretability in the wild: a circuit for indirect object identification in gpt-2 small, 2022.
 650

651 Jason Wei, Xuezhi Wang, Dale Schuurmans, Maarten Bosma, brian ichter, Fei Xia, Ed H. Chi,
 652 Quoc V Le, and Denny Zhou. Chain of thought prompting elicits reasoning in large language
 653 models, 2022.

654 Zichao Yang, Phil Blunsom, Chris Dyer, and Wang Ling. Reference-aware language models, 2017.

655 Eric Zelikman, Yuhuai Wu, Jesse Mu, and Noah Goodman. Star: Bootstrapping reasoning with
 656 reasoning, 2022.

658 Eric Zelikman, Georges Harik, Yijia Shao, Varuna Jayasiri, Nick Haber, and Noah D. Goodman.
 659 Quiet-star: Language models can teach themselves to think before speaking, 2024.

660 Dani Zhou, Enyu Zhou, Kevin Han, and Prashant Kambadur. Understanding chain-of-thought in
 661 llms through information theory, 2023.

663 A TRAINING STABILITY AND IMPLEMENTATION DETAILS

665 Fine-tuning a pre-trained language model with a strong linguistic prior requires careful consideration
 666 to avoid irrecoverable weight updates that could push the model out of the language modeling loss
 667 basin. We implement several techniques to enhance training stability for the GRPO objective:

669 **1. Low-Rank Adaptation (LoRA) (Hu et al., 2022):**

- 670 • Freeze all weights except for small-rank LoRA adapters.
- 671 • Use rank 8 with $\alpha = 16$.

672 **2. Gradient Clipping:**

- 673 • If the ℓ_2 norm of the gradient exceeds 1.0, rescale it to norm 1.0.

675 **3. Within-Batch Advantage Standardization:**

- 676 • GRPO’s parallel sampling enables robust within-batch standardization, eliminating
 the need for historical baselines.
- 678 • Each batch provides its own reference distribution for advantage calculation.

679 **4. Actor Reward Weight:**

- 680 • Set actor reward weight to 1.0 to equally balance policy gradient and direct reward
 optimization.
- 682 • This enables end-to-end learning through the reward model.

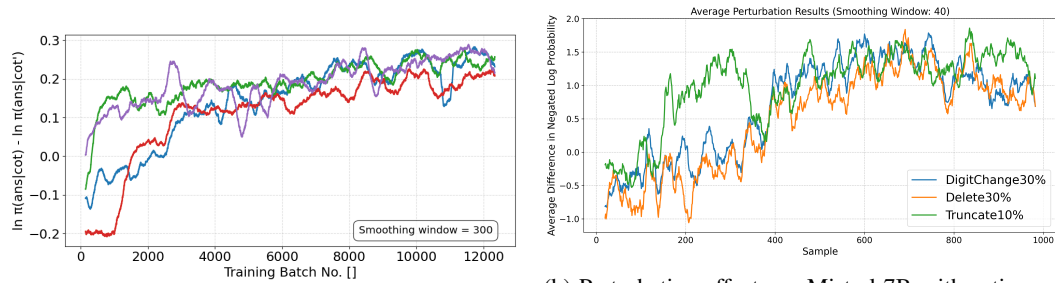
684 **5. Initial CoT Prompt Design:**

- 685 • Choose CoT_{init} to guide the model toward meaningful reasoning.
- 686 • For arithmetic:
 “You will be given an arithmetic problem, which you have [CoT length] tokens to work
 through step-by-step. Question.”
- 688 • For GSM8K:
 “You will be given a reasoning problem, which you have [CoT length] tokens to work
 through step-by-step. Question.”
- 691 • For Wikipedia continuation:
 “Compress your understanding of this text into [CoT length] tokens, then predict the
 next [target length] tokens.”

694 These measures greatly reduce the risk of catastrophic updates and keep the model’s training on
 695 track.

697 B ADDITIONAL PERFORMANCE ANALYSIS

700 This section presents additional performance metrics and analysis across our experimental settings.
 701 Fig 4a shows training progress on the Wikipedia continuation task, Fig 4b demonstrates perturbation
 effects on arithmetic reasoning, and Fig 3 illustrates cross-model transfer on GSM8K.



(a) Training progress on Wikipedia continuation task for Llama 8B, showing normalized improvement in next-token prediction across four independent runs.

(b) Perturbation effects on Mistral 7B arithmetic reasoning, showing three types of CoT modifications: digit changes, character deletions, and right truncation. Averaged over 4 PPO training runs.

Figure 4: Additional performance analysis across different tasks and metrics. (a) Training performance on Wikipedia. (b) Perturbation analysis on arithmetic.

C TRUTHFULNESS AND ELICITING LATENT KNOWLEDGE

Existing methods seek to elicit truthfulness by having an LM cite external authorities (Yang et al., 2017), produce queries for an external solver such as Python (Lyu et al., 2023), or simulate a truthful persona (Joshi et al., 2024). Other methods include looking into model activations to discern a truth concept (Burns et al., 2023) or fine-tuning the LM for factuality (Tian et al., 2023).

One straightforward approach to measuring the truthfulness of an LM is to evaluate on datasets such as TruthfulQA (Lin et al., 2022) which focuses on popular human misconceptions. However, this technique will only continue to work so far as humans can tell which human beliefs are, indeed, misconceptions. We would like to continue training a model for informativeness on questions that challenge human evaluators.

Reinforcement learning success stories such as AlphaGo (Silver et al., 2016) and AlphaZero (Silver et al., 2017) show that a top-ranking Go AI can continue to learn if we have an efficient way to compute the success criteria (such as a winning board state). However, many important success criteria are abstractions, and only exist within a person’s ontology. This problem is discussed at length in Christiano et al. (2021), and we will use their example to illustrate the situation.

Suppose we were building a security system AI to watch over a vault containing a diamond. Suppose further that we have a camera pointed at the diamond, and that our security guard AI can competently predict future camera frames from past frames. How can we train it to classify camera sequences according to the ambiguous human concept of whether the diamond is still in the room, even in difficult scenarios when a person would not be able to provide a ground truth label (e.g., subtle camera tampering)? If we train the classifier based on scenarios when a person can provide ground truth labels, then the AI’s video classifier has two valid generalization behaviors: (1) to say whether it thinks the diamond is still in the room and (2) to say whether the dataset-labeler would think the diamond is still in the room.

Our approach favors the second generalization behavior by using RL to train the AI to produce messages such that the person can themselves predict future camera frames. This idea is based on the following three insights:

- Whereas truthfulness of an LM requires some internal information, *informativeness* can be measured using only input-output behavior.
- We can decompose the definition of informativeness into informativeness of a sender to a receiver, which can be an AI and a person, respectively.
- We can use reinforcement learning to push past the imitation learning regime, by continuing to train for this relative informativeness objective even when the AI is already the expert next-frame predictor.

756 D TRAINING ALGORITHM IMPLEMENTATION AND COMPARISON 757

758 This section provides detailed descriptions of the reinforcement learning algorithms implemented in
759 our codebase for Markovian CoT training. Our core contribution is the Markovian training paradigm
760 that optimizes P(answer — CoT) rather than P(answer — question, CoT), creating a text bottleneck
761 where the CoT must be causally load-bearing. We implement multiple optimization approaches to
762 support this paradigm, enabling comprehensive algorithmic comparison.

764 D.1 ALTERNATE TRAINING ALGORITHMS TESTED 765

766 Our codebase implements four distinct reinforcement learning algorithms, each designed to optimize
767 the informativeness objective for Markovian CoT generation:

768 **Parallel Sampling with Batch Baseline:** Our main algorithmic approach, which uses standardized
769 batch-wise advantage estimates (mean=0, std=1) without exponential moving average baseline mix-
770 ing. This differs from standard GRPO by incorporating the Markovian reward constraint where the
771 same model parameters θ are used for both policy and reward calculation, eliminating the need for
772 iterative reward model updates.

773 We also implement three additional training objectives for algorithmic comparison:

775 **Policy Gradient (PG):** Uses the standard REINFORCE gradient with exponential moving average
776 baseline:

$$777 \mathcal{L}_{\text{PG}} = -\ln u_{\theta}(\text{CoT} \mid q, \text{CoT}_{\text{init}}) \cdot A^{\text{detach}} \quad (3)$$

779 where A is the advantage computed from the informativeness reward $R_{\theta} = \ln \pi_{\theta}(\text{ans} \mid \text{CoT}) -$
780 $\ln \pi_{\theta}(\text{ans} \mid \text{CoT}')$ and an exponential moving average baseline $V_t = \sum_{i=1}^{t-1} w_i R_i$ with weights
781 $w_i = r^{t-1-i} / \sum_{j=1}^{t-1} r^{t-1-j}$ (parameter $r = 0.9$).

782 **PPO-style Clipped Objective:** Uses the PPO clipping objective (not the full PPO algorithm) to
783 prevent large policy updates:

$$785 \mathcal{L}_{\text{PPO}} = -\min(r_t(\theta)A_t, \text{clip}(r_t(\theta), 1 - \epsilon, 1 + \epsilon)A_t) \quad (4)$$

787 where $r_t(\theta) = \frac{\pi_{\theta}(\text{CoT}_t)}{\pi_{\theta_{\text{old}}}(\text{CoT}_t)}$ is the probability ratio and $\epsilon = 0.2$ is the clipping parameter. Note this
788 applies clipping within our single-step framework rather than the multi-epoch data collection and
789 update scheme of standard PPO.

790 **Expert Iteration (EI):** Selectively trains only on high-reward examples above a dynamic threshold:

$$792 \mathcal{L}_{\text{EI}} = \mathcal{L}_{\text{PG}} \cdot \mathbb{I}[R_{\theta} > \tau_t] \quad (5)$$

793 where τ_t is computed as $\mu + k\sigma$ from the running history of rewards, with $k = 2.2$ standard devia-
794 tions in our experiments.

796 D.2 CROSS-MODEL INTERPRETABILITY ANALYSIS 797

798 Figure 5 presents the cross-model evaluation analysis that demonstrates the interpretability of CoT
799 generations across different model architectures. This analysis supports the interpretability claims
800 in the main paper by showing that learned reasoning patterns generalize across different language
801 model architectures rather than being model-specific artifacts.

802 The cross-model transferability shown in Figure 5 addresses the key question of “interpretable to
803 whom?” by demonstrating that trained CoTs transfer effectively across diverse model families,
804 confirming they contain generalizable reasoning patterns rather than model-specific artifacts.

806 E QUALITATIVE ANALYSIS OF GENERATED COTs 807

809 This section provides concrete examples of how Markovian training changes the character of gener-
ated CoT reasoning across different task domains.

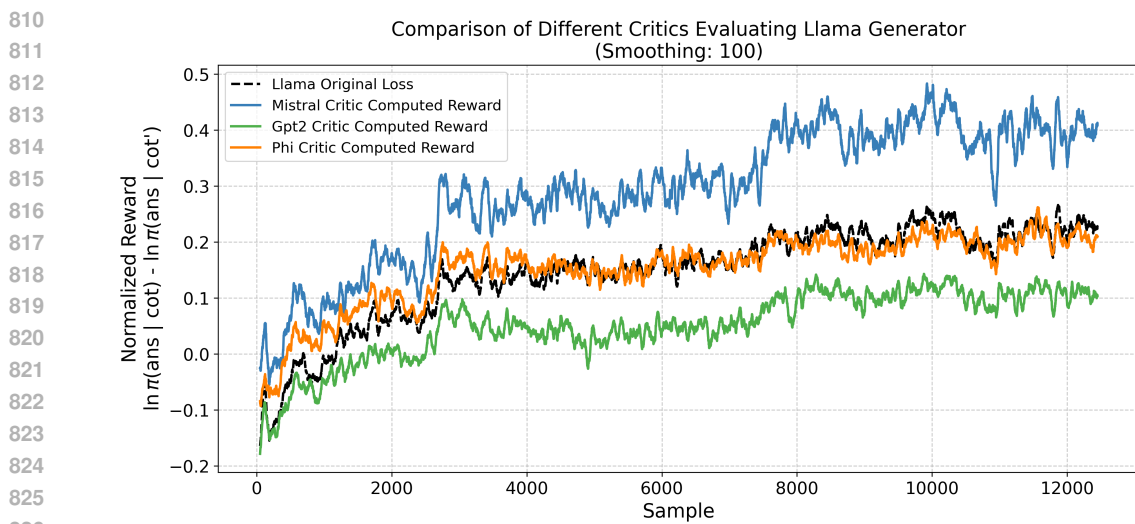


Figure 5: Cross-model evaluation showing Llama-3.1-8B-Instruct’s evaluation of Mistral’s CoT quality throughout training on Wikipedia text prediction. The correlation between improvements in both models’ evaluations suggests the learned reasoning patterns generalize across architectures rather than being model-specific artifacts. Each plot is averaged across 6 independent training runs.

E.1 ARITHMETIC TASK EXAMPLE

Here is an example from Llama-3.1-8B-Instruct on the arithmetic task (data: /root/MarkovianTraining/results/arithmetic/20250925_041804), showing the final actor and baseline reasoning sampled from the training log.

Batch Index 299

Question $1 + 47 + 35 + 58 + 92 + 19 + 37 + 94 + 30 + 81 + 30 + 1 + 66 + 92 + 78$

Actor Reasoning $1 + 47 = 48$. $48 + 35 = 83$. $83 + 58 = 141$. $141 + 92 = 233$. $233 + 19 = 252$. $252 + 37 = 289$. $289 + 94 = 383$. $383 + 30 = 413$. $413 + 81 = 494$. $494 + 30 = 524$. $524 + 1 = 525$. $525 + 66 = 591$. $591 + 92 = 683$. $683 + 78 = 761$. The answer is 761. Spoiler: to solve the problem, just add continuously, like a summarized version, to

Baseline Reasoning To solve this problem, you need to add the numbers together step by step. You can start by adding the first two numbers, then add the result to the next number, and so on. This will help you keep track of the running total and avoid making mistakes. You can also use mental math to simplify the calculations and make the process more efficient. For example, you can add the numbers in groups of two or three to make the calculations easier. Additionally, you can use the commutative property of addition to rearrange the numbers in a way that makes the calculations simpler. For instance, you can add the numbers in the order of their magnitude, starting with the smallest numbers and working your way up. This will help you avoid having to

Answer 761

E.2 WIKIPEDIA CONTINUATION EXAMPLE

To better understand Llama-3.1-8B-Instruct’s behavior after Markovian training to predict Wikipedia text, let’s examine its behavior on the (randomly selected near the end of training) batch number 12500. The model was given the following Wikipedia article excerpt:

Boones Mill is a town in Franklin County, Virginia, United States. The population was 239 in 2018, down from 285 at the 2000 census. It is part of the Roanoke Metropolitan Statistical Area.

History

Boones Mill was incorporated in 1927. It was previously known as “Boone Mill”

864 and "Boon Mill". The town is named after Jacob Boon who operated a mill in the
 865 town.

866 The Boones Mill Norfolk & Western Railway Depot is listed on the National Register
 867 of Historic Places. <https://www.townofboonesmill.org/history>

868 **Geography**

869 Boones Mill is located in northern Franklin County at (37.115462, -79.953966),
 870 along U.S. Route 220 at the southern base of the Blue Ridge Mountains. US 220
 871 leads north to Roanoke and south to Rocky Mount, the Franklin County seat.

872 According to the United States Census Bureau, the town has

873
 874 Given this context ending with "According to the United States Census Bureau, the town has", we
 875 can compare the CoT generated by our trained versus an untrained model:

876
 877 **E.2.1 COT AFTER TRAINING:**

878 "The town of Boones Mill is located in Franklin County, Virginia, United States.
 879 US 220 leads north to Roanoke and south to Rocky Mount, the Franklin County
 880 seat. According to the United States Census Bureau, the town has"

881
 882 **E.2.2 COT BEFORE TRAINING:**

883 "The town of Boones Mill is a small, rural community with a rich history and natural
 884 beauty. The town is surrounded by the Blue Ridge Mountains, offering scenic
 885 views and outdoor recreational opportunities. The town's economy is primarily
 886 based on agriculture and small"

887
 888 **E.2.3 ACTUAL CONTINUATION:**

889 "a total area of , all of it land. The town is in the valley of Maggodee Creek,
 890 a southeast-flowing tributary of the Blackwater River, part of the Roanoke River
 891 watershed. Murray Knob, elevation , rises to the north on the crest of the Blue
 892 Ridge, and the eastern end of Cahas Mountain, at , is 2 miles to the west."

893 The trained CoT shows notably different characteristics from the untrained one. The trained CoT
 894 essentially copied the first and last two sentences from the context, making sure to line up the number
 895 of allotted tokens with the end of the last sentence. The untrained model seems to give fairly generic
 896 properties that the actual Boones Mill Wikipedia article does not mention, such as Boones Mill
 897 having an economy primarily based on agriculture. Also, the untrained CoT is not taking the token
 898 limit into account and is setting the evaluator model to be surprised when it glues the CoT to the
 899 answer and has to predict "agriculture and small a total area of , all of it land".

900 This example achieved a normalized reward of 0.3438 (in log probability), suggesting that the trained
 901 CoT strategy was indeed helpful for predicting the technical geographic description that followed.

902
 903 **F HYPERPARAMETER TUNING AND EXPERIMENTAL CONFIGURATIONS**

904 Our Wikipedia continuation experiments systematically explored the hyperparameter space across
 905 multiple model architectures and training configurations. Table 2 reports the maximum smoothed
 906 normalized reward for each configuration, computed using a 100-batch moving average window to
 907 reduce noise while preserving trend information. This approach captures peak performance before
 908 potential saturation or divergence, providing a more robust comparison than final batch values.

909 The experimental design explored several key dimensions:

910 **Model Architecture:** We evaluated four different language models (Llama, Mistral, Phi, and
 911 Qwen3) to assess the generalizability of our Markovian training approach across different archi-
 912 tectures and parameter scales.

913 **Temperature Scaling:** We systematically varied the sampling temperature (1.2, 1.3, 1.4) to study
 914 the effect of generation diversity on Markovian training effectiveness. Higher temperatures (1.4)

918 consistently achieved better results than lower temperatures, encouraging more diverse CoT generation
 919 and robust reasoning patterns.
 920

921 **Markovian vs Non-Markovian Training:** For each model and temperature combination, we con-
 922 ducted paired experiments comparing Markovian training (Markov=Y) versus Non-Markovian train-
 923 ing (Markov=N) to isolate the effects of our approach. As expected, Non-Markovian models achieve
 924 approximately $2\times$ higher normalized rewards because they can access both the question and CoT
 925 during answer generation. However, this performance advantage comes at the cost of interpretabil-
 926 ity, as demonstrated in our perturbation analysis (Table 1).
 927

928 **Batch Size Optimization:** Batch sizes were tailored to each model’s memory requirements and
 929 computational efficiency, ranging from 6 (Mistral, Llama) to 16 (Phi) based on GPU memory con-
 930 straints and convergence characteristics.
 931

932 **Parallel vs Non-Parallel Training:** Parallel training (GRPO-style batch-based advantage estima-
 933 tion) dramatically outperformed non-parallel training (Expert Iteration with exponential moving
 934 average baseline) by $10\text{--}30\times$. Non-parallel runs often achieved near-zero or negative maximum
 935 rewards, demonstrating that GRPO is essential for stable Markovian training on this task.
 936

937 Table 2: Wikipedia continuation experiments showing maximum smoothed normalized reward (100-
 938 batch moving average). Non-Markovian models achieve higher maxima because they can access
 939 both question and CoT during answer generation, but at the cost of interpretability. Runs marked
 940 with * were used in Figure 2.

Model	Temp	Batch	Par.	Mar.	Max Reward
llama	1.2	6	N	Y	-0.165
llama	1.2	6	Y	N	+0.040
llama	1.3	8	Y	Y	+0.140*
mistral	1.3	10	N	Y	+0.139
mistral	1.4	6	Y	Y	+0.337*
mistral	1.4	6	Y	N	+0.632
phi	1.3	16	N	Y	-0.005
phi	1.4	16	Y	Y	+0.267*
phi	1.4	16	Y	N	+0.424
qwen3	1.3	12	N	Y	+0.103
qwen3	1.4	12	Y	Y	+0.327*
qwen3	1.4	12	Y	N	+0.124

955 **Key Findings.** The results reveal several important patterns. First, Non-Markovian models con-
 956 sistently achieve approximately $2\times$ higher maximum rewards (mean: +0.305) compared to Markovian
 957 models (mean: +0.143), confirming that access to both question and CoT during answer generation
 958 substantially eases the prediction task. However, this performance advantage comes at the cost of
 959 interpretability—our perturbation analysis (Table 1) demonstrates that Markovian models exhibit
 960 52%–82% higher sensitivity to CoT modifications, confirming their CoTs are more causally load-
 961 bearing.

962 Second, parallel training (GRPO) dramatically outperforms non-parallel training (Expert Iteration).
 963 Non-parallel runs achieve near-zero or negative maximum rewards (mean: +0.018), while parallel
 964 runs show robust positive improvements (mean: +0.286). This $16\times$ difference demonstrates that
 965 GRPO-style batch-based advantage estimation is essential for stable Markovian training.
 966

967 Third, the four Markovian parallel runs (marked with *) achieve maximum rewards ranging from
 968 +0.140 to +0.337, with Mistral performing best, followed by Qwen3, Phi, and Llama. These
 969 represent solid improvements while maintaining the interpretability benefits of Markovian training.

970 The systematic exploration of this hyperparameter space enabled robust evaluation of our Markovian
 971 training approach and provided confidence in the generalizability of our results across different
 972 model architectures and training configurations.

972 **G IMPACT STATEMENT**
973

974 Reinforcement learning techniques improve a policy with respect to an arbitrary reward function.
975 But it can be difficult to mathematically specify nuanced human preferences about the policy. Both
976 reinforcement learning from human feedback (RLHF) (Christiano et al., 2023) and Constitutional
977 AI (Bai et al., 2022) help people specify and optimize the properties they would like the AI to have.
978 This increase in controllability makes the AI more of an extension of human intention, for better or
979 for worse. The approach of this paper is much more targeted – we use RL to specifically increase an
980 agent foresight – its ability to predict its future observations.

981 On its face, this seems like it might be just as dependent on human intentions as RLHF and Constitu-
982 tional AI – if an LM is more knowledgeable, maybe it could use that extra knowledge to deceive
983 others, for instance. However, better foresight may also give rise to better values, where values are
984 opinions about how to act such that the collective system can attain better foresight.

985
986
987
988
989
990
991
992
993
994
995
996
997
998
999
1000
1001
1002
1003
1004
1005
1006
1007
1008
1009
1010
1011
1012
1013
1014
1015
1016
1017
1018
1019
1020
1021
1022
1023
1024
1025